Supplementary Information

Copper hydroxide/Basic copper salt derived Cu with Clear grain boundary for selectively electrocatalytic CO_2 reduction to multicarbon products

Shuchang Song,‡[a] Haoyang Wu,‡[a] Benqiang Tian,[a] Ying Zhang*[b], Yun Kuang*[ac] and Xiaoming Sun[a]

[a]State Key Laboratory of Chemical Resource Engineering, College of Chemistry, Beijing University of Chemical Technology, Beijing 100029, P.R. China.

[b]Key Laboratory of Synthetic and Biological Colloids, Ministry of Education, School of Chemical and Material Engineering, Jiangnan University, Wuxi, 214122, China.

[c]Ocean Hydrogen Energy R&D Center, Research Institute of Tsinghua University, Shenzhen 518057, P.R. China.

‡ These authors contributed equally to this work.

*Corresponding Author(s): kuangy@tsinghua-sz.org; ying.zhang@jiangnan.edu.cn

1. Experimental Procedures

1.1 Materials and chemicals

copper sulfate pentahydrate ($CuSO_4 \cdot 5H_2O$, 99.999%), deuteroxide (D_2O) and dimethyl sulfoxide (DMSO) were purchased form Alfa Aesar. Ammonia ($NH_3 \cdot H_2O$, AR) and sodium hydroxide (NaOH, AR) was purchased from Xilong chemical industry. Potassium iodide (KI, 99.99%), potassium sulfate (K_2SO_4, 99.99%), copper nitrate hydrate ($Cu(NO_3)_2 \cdot 3H_2O$, 99.99%), copper dichloride ($CuCl_2$, 99.99%) and sodium carbonate (Na_2CO_3, 99.999%) were purchased form Aladdin. Carbon dioxide (CO_2, 99.99%) and nitrogen (N_2, 99.99%) were purchased from Bejing Huatong Jingke Chemical Co., Ltd.

1.2 Physicochemical characterizations

The microscopic surface structure of the samples was observed and analyzed by SEM (Zeiss SUPRA), of which the working voltage is 20 KV and the acceleration voltage is 5000 V. The TEM (FEI Tecnai G2 20 STwin) was used to analyze the fine structure of the catalysts before and after ECR test, where the catalysts-loaded carbon substrate after ECR test were quickly cut into ethanol condition for ultrasound, after ten minutes, the dispersion of catalysts was dropped on copper mech, which was dried carefully under infrared lamp for TEM analysis. HR-TEM (JEOL JEM-2100) was used to analysis the microscopic morphology and lattice fringes of samples. When preparing samples for HR-TEM test, the dispersion mentioned above was dropped onto molybdenum mesh, which was dried carefully under infrared lamp for testing. As for the structure analysis by mean of AC-TEM (Themis Z), the method of sample preparation and protection was the same as that in HR-TEM. The whole time before testing should make sure that the sample stored in inert gases condition to avoid it being oxidized.

The phase composition, lattice, structure and other information of the samples were analyzed by some other instruments as well. X-ray diffraction spectrometer (MeasSrv F9XDZ42) was used to analyze the crystal composition of our catalysts, where the scanning range (2 theta) was 5°~80° and the scanning speed was 2°/min. And before test, the sample after ECR test should be stored under inert gases condition for protection. In situ XPS was used for Cu valence analysis, notice that the catalysts after ECR test should be stored under inert gases condition to avoid the sample being oxidized as well.

1.3 Catalysts synthesis and cathode preparation.

$Cu(OH)_2$/BCS-S: 30 mL ammonia aqueous solution (0.15 M) was added into 20 mL copper sulfate aqueous solution (0.2 M) under constant stirring for 15 minutes, during which the blue solution gradually became green dispersion. After that, 2.88 mL NaOH aqueous solution with different concentrations was added into above dispersion under constant stirring for another 15 minutes. Then the dispersion was collected and washed by deionized water and ethanol for several times, the products were finally frozen and put into vacuum freezing dryer for 12 hours.

$Cu(OH)_2$/BCS-N: We adopted the synthesis method of BCS-N reported by Sun et al.[1] Typically, there-necked flask containing 20 mL copper nitrate aqueous solution (3.5 M) was heated to boil in oil bath, then 50 mL NaOH aqueous solution (0.7 M) was dropped into above solution under constant stirring. After constant stirring for 10 minutes, the solution was cooled naturally, collected and wash by deionized water and ethanol for several times, then the products was frozen and dried in vacuum freezing drier for 12 hours. After that, a solution containing 300 mg above powder and 5 mL deionized water was added by NaOH aqueous solution with different concentrations under constant stirring for 15 minutes, the products were then collected, washed by deionized water and ethanol, frozen and dried in vacuum freezing drier for 12 hours.

$Cu(OH)_2$/BCS-Car: 10 mL copper sulfate aqueous solution (0.5 M) was dropped into 12 mL sodium carbonate aqueous solution (0.5 M) under constant stirring for 15 minutes, which was then heated at 75 ℃ in boil bath for 15 minutes, the blue solution would turn to green gradually. The products were then washed by deionized water and ethanol for several times, frozen and dried in vacuum freezing drier for 12 hours. After that, a solution containing 100 mg above products and 10 mL deionized water was added by NaOH aqueous solution with different concentrations under constant stirring for 15 minutes, the final products were collected, washed by deionized water and ethanol, frozen, dried in vacuum freezing drier for 12 hours.

$Cu(OH)_2$/BCS-Ch: We adopted the synthesis method of BCS-Ch reported by Xue et al.[2] Typically, 0.74 g NaOH was dissolved in 20 mL deionized water (solution A), 2.10 g $CuCl_2$ was dissolved in 20 mL deionized water (solution B), the solution A was dropped into solution under constant stirring for 10 minutes, which was then heated at 70 ℃ in oil bath for 40 minutes, the products was then washed by deionized water ethanol, frozen, dried in vacuum freezing drier for 12 hours. After that, the solution containing 100 mg above products and 10 mL deionized water was added by NaOH

aqueous solution under constant stirring for 15 minutes, which was then collected, washed by deionized water and ethanol, frozen, dried in vacuum freezing drier for 12 hours.

Cathode preparation: The ink containing 3 mg catalysts, 1 mL ethanol and 5 μL nafion solution (5%) was under ultrasound for one hour to obtain a well dispersed ink. The hydrophobic carbon paper (1×3 cm^2) was applied for substrate after carefully washed by hydrochloric acid, acetone and deionized water solution for three times, respectively. Then, 80 μL above ink was drop coated onto carbon substrate and dried under infrared lamp, which was prepared for the following ECR test.

1.4 Electrochemical test system

All electrochemical performance tests in this paper (LSV, CV, EIS, etc.) were carried out under ambient temperature and pressure condition with a three-electrode system, where the working electrode was catalysts supported by carbon substrate, the reference electrode was Ag/AgCl electrode, and graphite rod was adopted for counter electrode, H-type electrolytic cell for reaction vessel. 13 ml of 1 M KI aqueous solution was added to the cathodic electrolytic cell, an equal volume of 0.5 M K_2SO_4 electrolyte was added to the anodic electrolytic cell, and a Nafion115 proton exchange membrane (after being soaked in 0.1 M $KHCO_3$ for 2 h) was placed between the two electrolytic cells. Before electrochemical testing, keep CO_2 gas flowing into the cell for 30 minutes to saturation.

1.5 ECR products analysis

The flow rate of CO_2 was maintained at 20 sccm by a mass flow controller, and CV and LSV tests were performed after that for 30 min. The potentiostatic polarization test was performed by selecting an appropriate potential from the current-potential curve diagram. The gas phase and liquid phase products were qualitatively and quantitatively analyzed by gas chromatography and liquid phase nuclear magnetic resonance spectroscopy, respectively. In this paper, the gas phase products are mainly H_2, CO, CH_4, C_2H_4 and the liquid phase products are mainly HCOOH, C_2H_5OH, C_3H_7OH.

The gas-phase products in CO_2 reduction flow from the cathode chamber entered the gas chromatograph (GC-2014 C, Shimadzu, Japan) for online detection. The products were determined according to the retention time of the peak positions of different products, and the content of the products was determined according to the area of the integrated peak. The composition and content of the liquid-phase products generated by ECR were detected by nuclear magnetic resonance spectrometer (AV400,

Bruker). For sample preparation, draw 500 μL of catholyte and add 100 μl internal standard (0.01% DMSO in D_2O). The contents of the products were calculated by comparing the peak area of the products with the peak area of DMSO.

The products of electrocatalytic CO_2 reduction are generally not single, and different products have different numbers of transferred electrons. In order to truly evaluate the selectivity difference of catalysts, the Faradaic Efficiency (FE) of different products is usually applied to represent the selectivity of catalysts in ECR. In this paper, the Faradaic efficiency of the product (x) is calculated by the following formula:

$$FE_x = \frac{Q_{towards\ x}}{Q_{total}} \times 100\%$$

Where $Q_{towards\ x}$ represent the electric charge for generating x from CO_2, and Q_{total} represent the total electric charge.

2. Supplementary Figures and tables

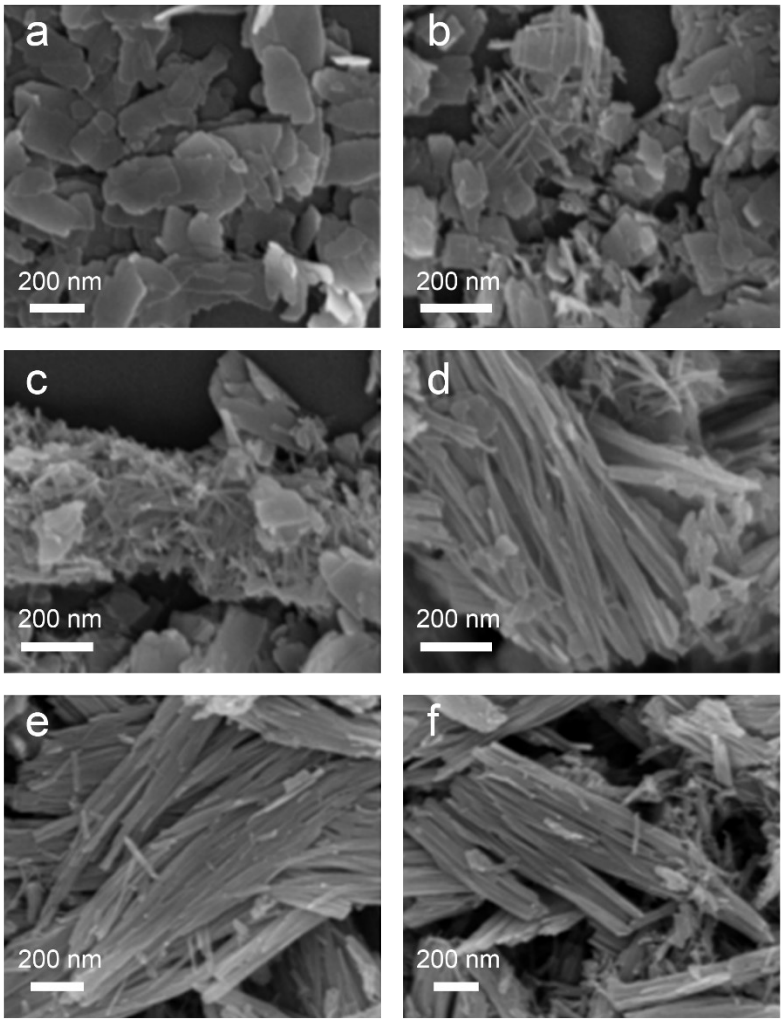

Figure S1. SEM of BCS-S manipulated with increased amount of NaOH. (a) 0 mmol, (b) 2 mmol, (c) 4 mmol, (d) 6 mmol, (e) 8 mmol and (f) 12 mmol.

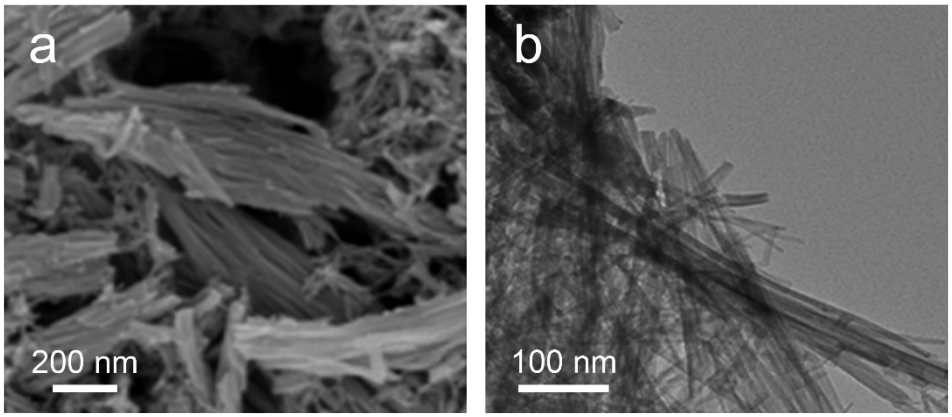

Figure S2. (a) SEM and (b) TEM of BCS-S manipulated with 7 mmol NaOH ($Cu(OH)_2$/BCS-S).

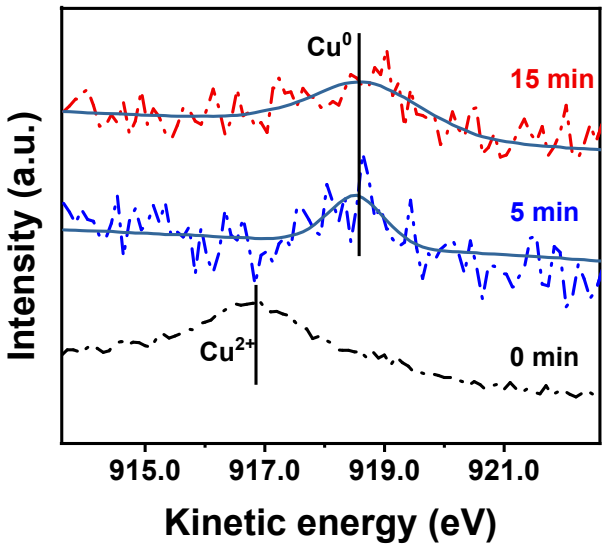

Figure S3. In situ Cu LMM energy spectrum (including primary data) of $Cu(OH)_2$/BCS-S at -1.2 V vs. RHE.

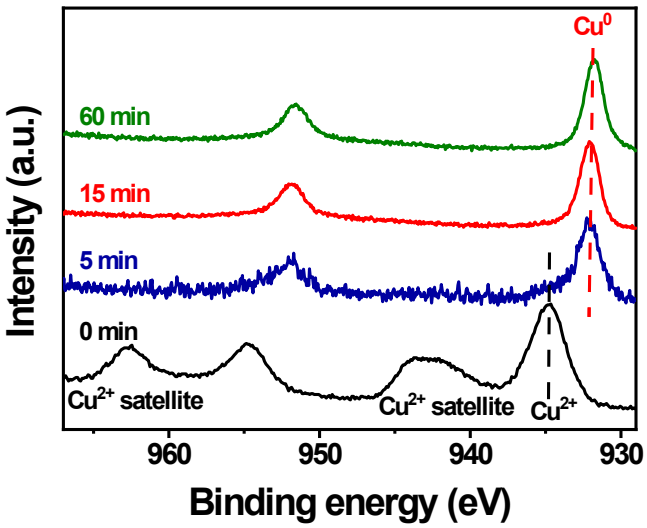

Figure S4. In situ Cu 2p energy spectrum of $Cu(OH)_2$/BCS-S at -1.2 V vs. RHE.

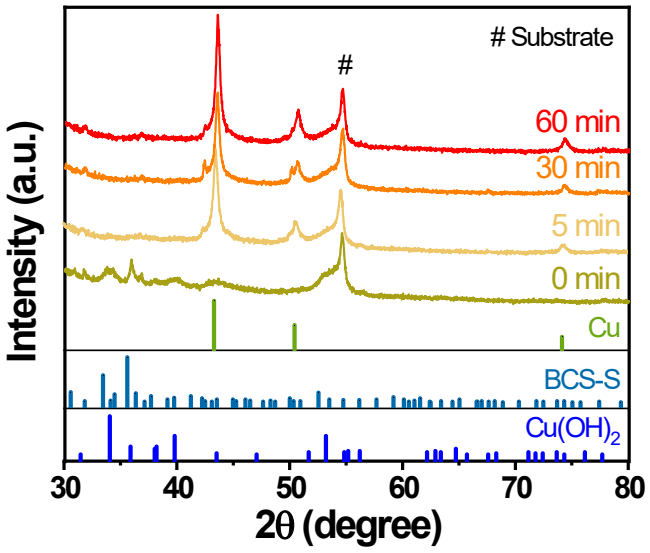

Figure S5. XRD of $Cu(OH)_2$/BCS-S after different ECR tests at -1.2 V vs. RHE.

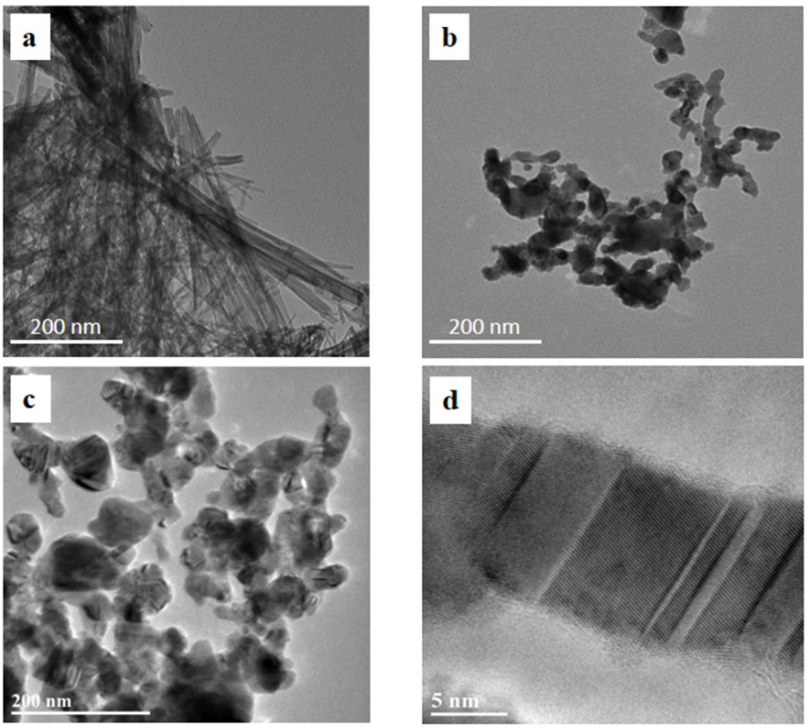

Figure S6. Structure evolution of $Cu(OH)_2$/BCS-S after 5 minutes ECR tests at -1.2 V vs. RHE. (a) TEM before ECR. (b) TEM, (c) HR-TEM and (d) AC-TEM after ECR.

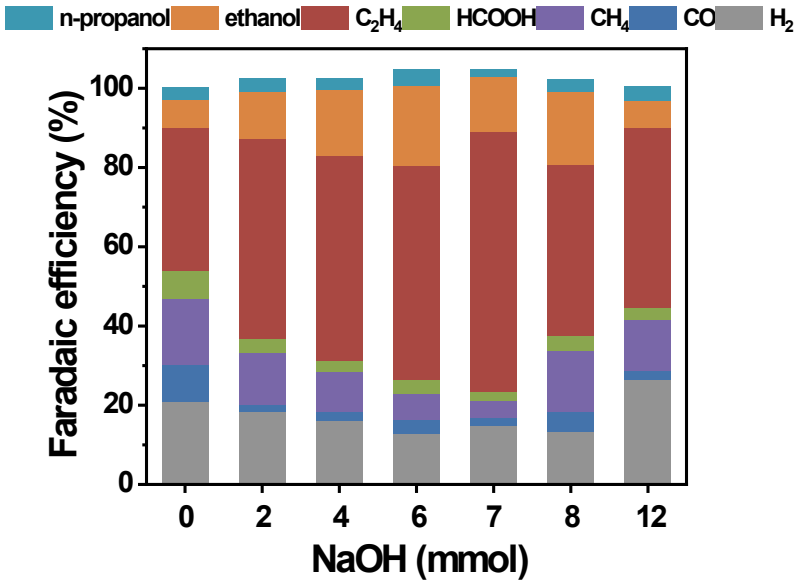

Figure S7. Products distribution of BCS-S manipulated with different amounts of NaOH after an hour ECR test at -1.2 V vs. RHE**.**

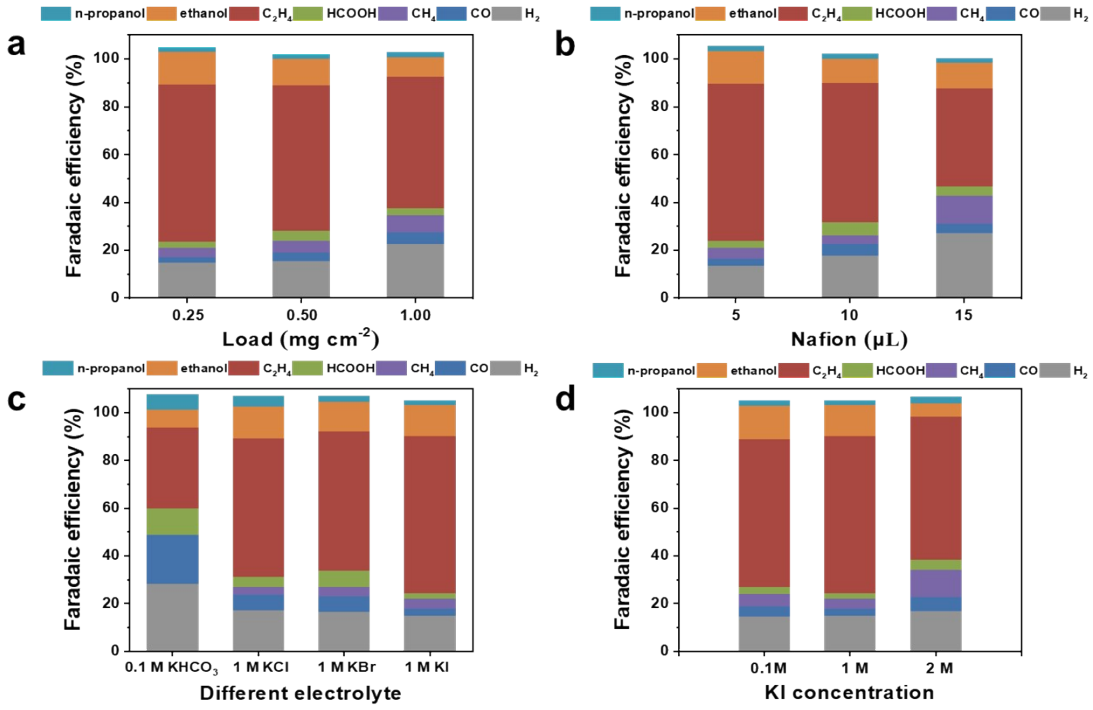

Figure S8. Products distribution of $Cu(OH)_2$/BCS-S under various testing parameters after an hour ECR test at -1.2 V vs. RHE. (a) catalysts loading. (b) dosage of nafion in catalysts ink preparation. (c) different catholytes. (d) different concentrations of KI catholyte.

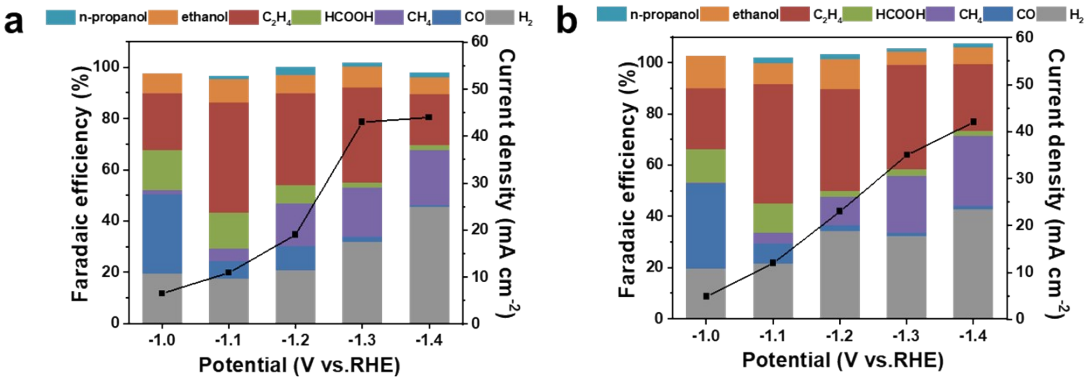

Figure S9. Products distribution of (a) BCS-S and (b) $Cu(OH)_2$-S at different potentials after an hour ECR test.

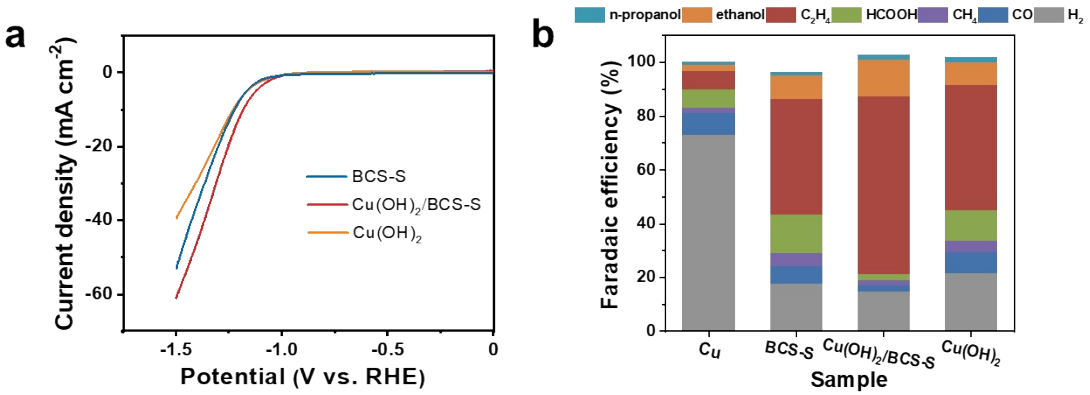

Figure S10. LSV of BCS-S, $Cu(OH)_2$/BCS-S and $Cu(OH)_2$-S at a scan rate of 5 mV/s. (b) Products distribution of Cu, BCS-S, $Cu(OH)_2$/BCS-S and $Cu(OH)_2$-S at their corresponding optimal potentials towards C_{2+} products after an hour ECR.

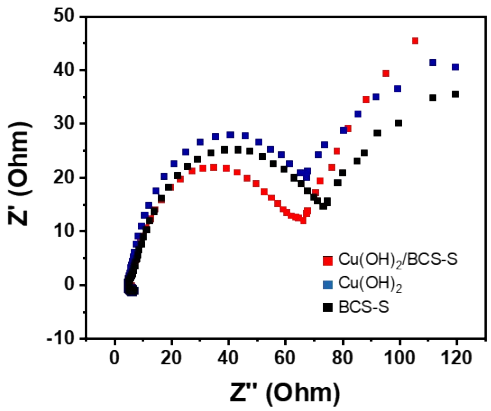

Figure S11. Electrochemical impedance spectroscopy (EIS) of BCS-S, $Cu(OH)_2$/BCS-S and $Cu(OH)_2$-S.

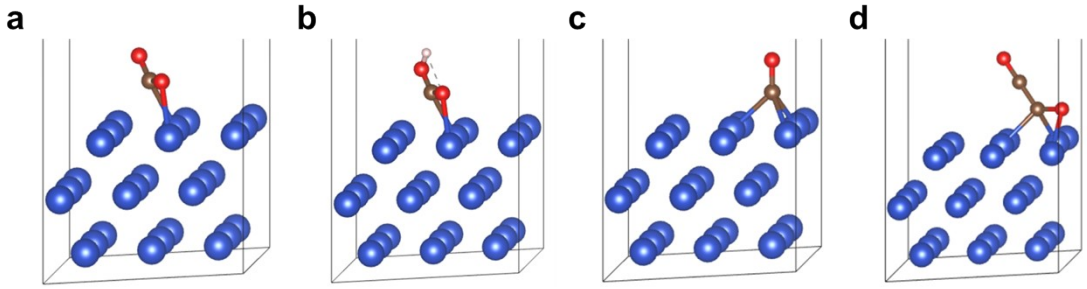

Figure S12. Optimized structure evolution of involved reaction coordinates on Cu(111).

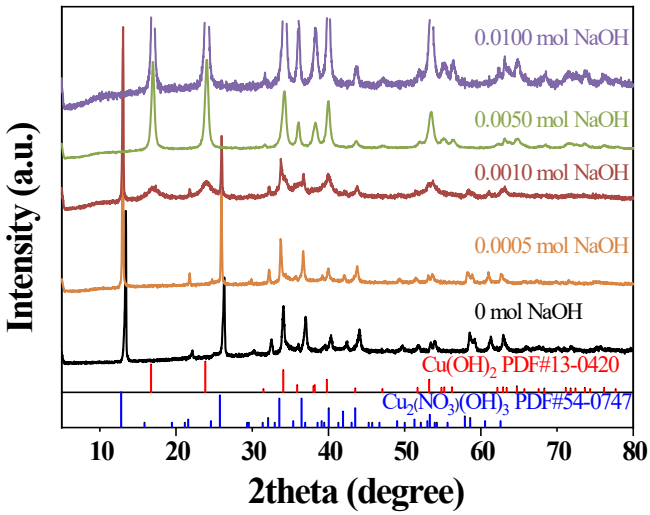

Figure S13. XRD of BCS-N manipulated with different amounts of NaOH.

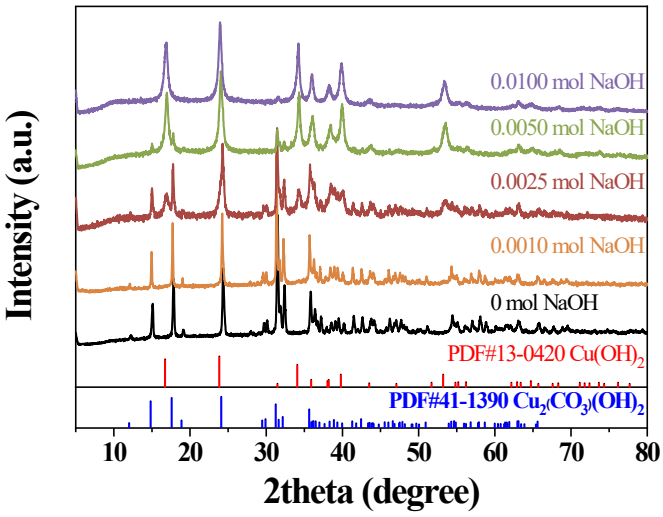

Figure S14. XRD of BCS-Car manipulated with different amounts of NaOH.

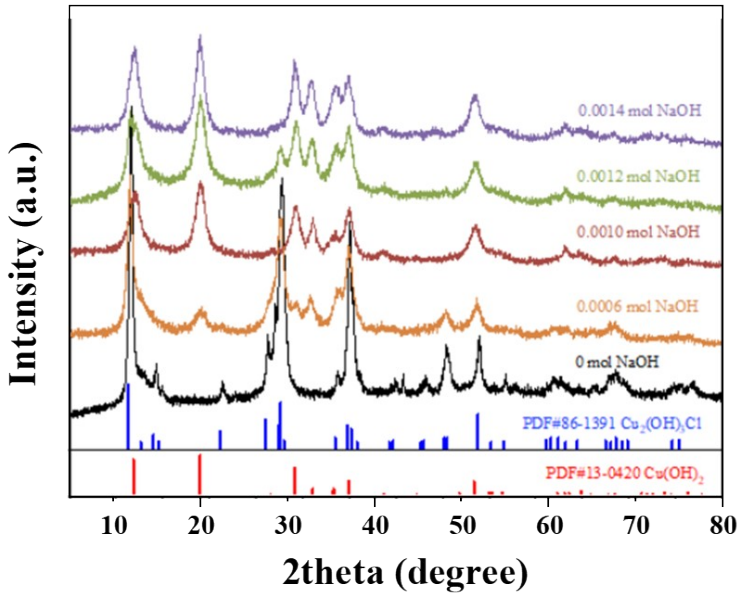

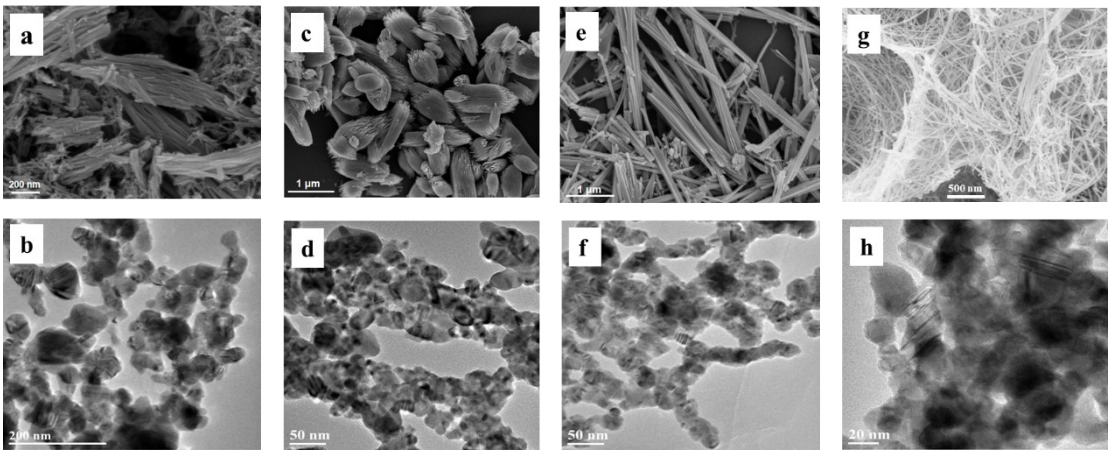

Figure S15. XRD of BCS-Ch manipulated with different amounts of NaOH.

Figure S16. Electron microscope of the four $Cu(OH)_2$/BCS. SEM of (a) $Cu(OH)_2$/BCS-S, (c) $Cu(OH)_2$/BCS-N, (e) $Cu(OH)_2$/BCS-Car and (g) $Cu(OH)_2$/BCS-Ch. HR-TEM of (b) $Cu(OH)_2$/BCS-S, (d) $Cu(OH)_2$/BCS-N, (f) $Cu(OH)_2$/BCS-Car and (h) $Cu(OH)_2$/BCS-Ch.

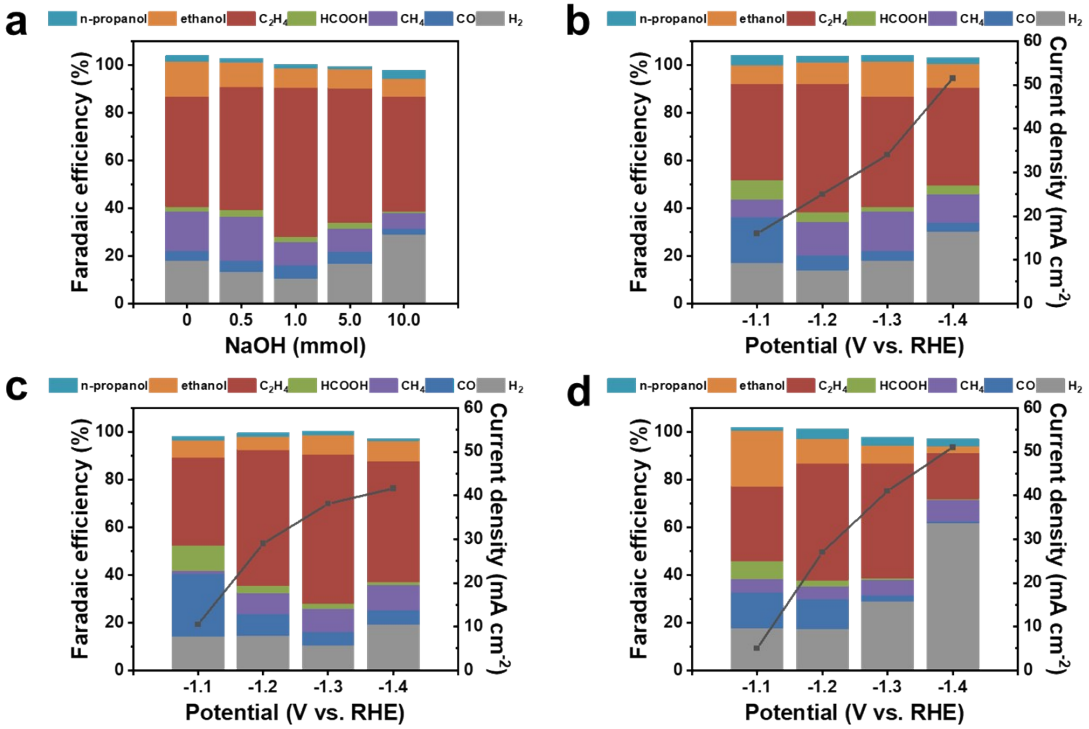

Figure S17. (a) Products distribution of BCS-N manipulated with different amounts of NaOH after an hour ECR at -1.3 V vs. RHE. Products distribution of (b) BCS-N, (c) $Cu(OH)_2$/BCS-N and (d) $Cu(OH)_2$-N after an hour ECR at different potentials.

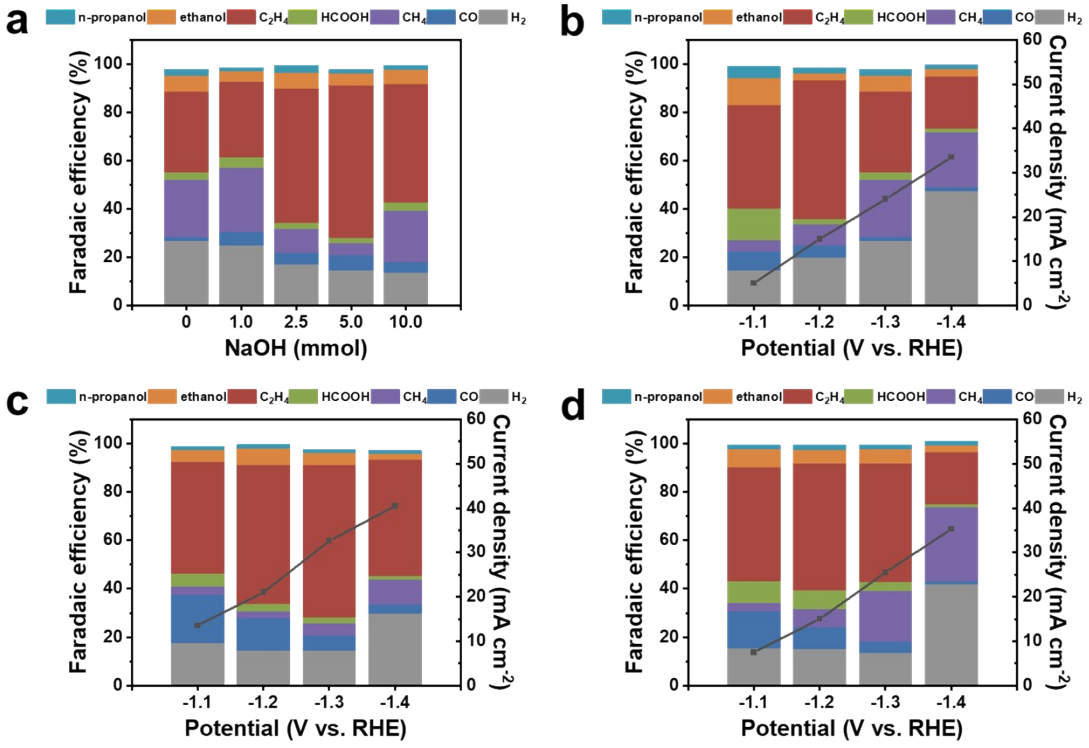

Figure S18. (a) Products distribution of BCS-Car manipulated with different amounts

of NaOH after an hour ECR at -1.3 V vs. RHE. Products distribution of (b) BCS-Car, (c) $Cu(OH)_2$/BCS-Car and (d) $Cu(OH)_2$-Car after an hour ECR at different potentials.

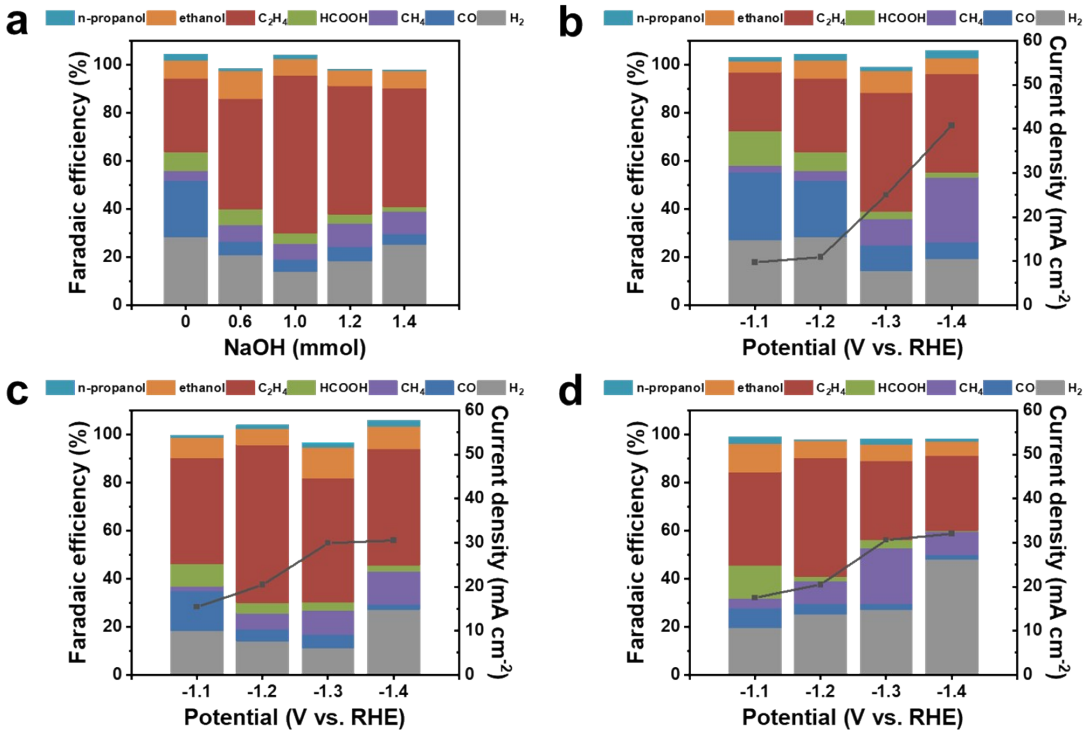

Figure S19. (a) Products distribution of BCS-Ch manipulated with different amounts of NaOH after an hour ECR at -1.2 V vs. RHE. Products distribution of (b) BCS-Ch, (c) $Cu(OH)_2$/BCS-Ch and (d) $Cu(OH)_2$-Ch after an hour ECR at different potentials.

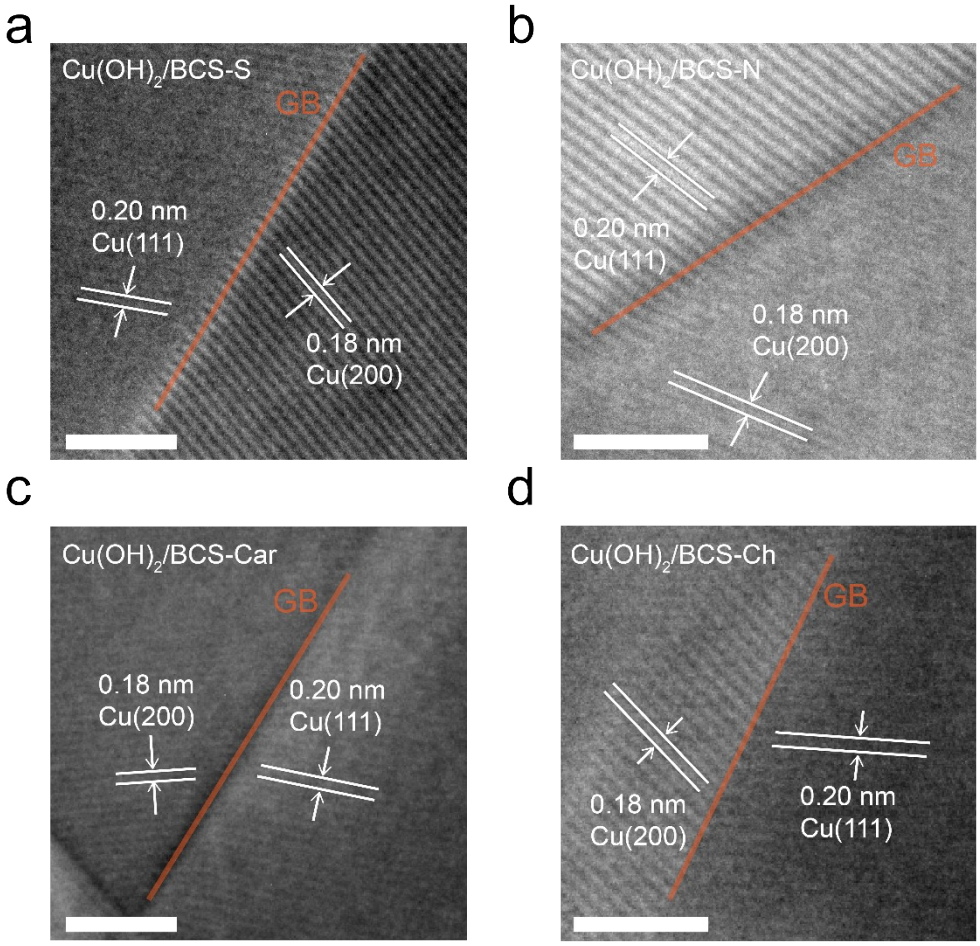

Figure S20. Denoted Cu^0 Grain boundary (Cu [*n*(200)×(111) step sites]) in the four $Cu(OH)_2$/BCS derived Cu. Scale bars: 2 nm.

Table S1. Detailed total geometric current density and faradaic efficiency of various products for the four $Cu(OH)_2$/BCS at their corresponding optimal potentials.

Sample	Potential (V vs. RHE)	J (mA cm^{-2})	H_2	CO	CH_4	HCOOH	C_2H_4	C_2H_5OH	C_3H_7OH
$Cu(OH)_2$/BCS-S	-1.2	30.2	14.6	2.2	2.1	2.4	65.7	13.9	1.7
$Cu(OH)_2$/BCS-N	-1.3	38.1	10.5	5.7	9.5	2.4	62.5	8.1	1.4
$Cu(OH)_2$/BCS-Car	-1.3	32.6	14.5	6.4	5	2.3	63.2	5	1.4
$Cu(OH)_2$/BCS-Ch	-1.2	29.9	14.1	4.9	6.8	4.4	65.6	6.8	1.5

Table S2. Comparison ECR performance of the four $Cu(OH)_2$/BCS with state-of-the-art Cu-based catalysts evaluated in H-type Cell[3-12].

Catalyst	Cell type	Catholyte	E (vs. RHE)	FE of C_{2+} (%)	J_{C2+} (mA cm^{-2})	Ref.
$Cu(OH)_2$/BCS-S	H-Cell	1 M KI	-1.2	81.3	24.55	This work
$Cu(OH)_2$/BCS-N	H-Cell	1 M KI	-1.3	72	27.43	This work
$Cu(OH)_2$/BCS-Car	H-Cell	1 M KI	-1.3	69.6	22.69	This work
$Cu(OH)_2$/BCS-Ch	H-Cell	1 M KI	-1.2	73.9	22.1	This work
Cu@NxC	H-Cell	0.1 M KHCO3	-1.1	76.8	14.9	3
Cu-s	H-Cell	0.1 M KHCO3	-1.1	55.8	26.69	4
p-Cu	H-Cell	0.1 M KHCO3	-1.3	57.2	22.65	5
CuO-CeO_2/CB	H-Cell	0.1 M KHCO3	-1.1	50	3.77	6
5-Ag/Cu_2O	H-Cell	0.1 M KHCO3	-0.98	65	6.09	7
Cu/$CuSiO_3$	H-Cell	0.1 M KHCO3	-1.10	60.64	12.25	8
Cu GNC-VL	H-Cell	0.5 M KHCO3	-0.87	70.5	7.33	9
Cu_3N	H-Cell	0.1 M CsHCO3	-1.00	68	12.58	10
CuBr-DDT	H-Cell	0.1 M KCl	-1.25	72	9.02	11
Cu/PANI	H-Cell	0.1 M KHCO3	-1.20	66	14.9	12

Reference

1. N. Ba, L. Zhu, H. Li, G. Zhang, J. Li and J. Sun, *Solid State Sci.*, 2016, **53**, 23-29.
2. K. Chen and D. Xue, *J. Phys. Chem. C*, 2013, **117**, 22576-22583.
3. Z. Li, Y. Yang, Z. Yin, X. Wei, H. Peng, K. Lyu, F. Wei, L. Xiao, G. Wang, H. D. Abruña, J. Lu and L. Zhuang, *ACS Catal.*, 2021, **11**, 2473-2482.
4. C. He, D. Duan, J. Low, Y. Bai, Y. Jiang, X. Wang, S. Chen, R. Long, L. Song and Y. Xiong, *Nano Res.*, 2021, **16**, 4494–4498.
5. B. Liu, C. Cai, B. Yang, K. Chen, Y. Long, Q. Wang, S. Wang, G. Chen, H. Li, J. Hu, J. Fu and M. Liu, *Electrochim. Acta*, 2021, **388**.
6. S. Chu, X. Yan, C. Choi, S. Hong, A. W. Robertson, J. Masa, B. Han, Y. Jung and Z. Sun, *Green Chem.*, 2020, **22**, 6540-6546.
7. A. Herzog, A. Bergmann, H. S. Jeon, J. Timoshenko, S. Kuhl, C. Rettenmaier, M. Lopez Luna, F. T. Haase and B. Roldan Cuenya, *Angew. Chem. Int. Ed.*, 2021, **60**, 7426-7435.
8. X. Yuan, S. Chen, D. Cheng, L. Li, W. Zhu, D. Zhong, Z. J. Zhao, J. Li, T. Wang and J. Gong, *Angew. Chem. Int. Ed.*, 2021, **60**, 15344-15347.
9. Y. Zhang, K. Li, M. Chen, J. Wang, J. Liu and Y. Zhang, *ACS Appl. Nano Mater.*, 2019, **3**, 257-263.
10. M. Ebaid, K. Jiang, Z. Zhang, W. S. Drisdell, A. T. Bell and J. K. Cooper, *Chem. Mater.*, 2020, **32**, 3304-3311.
11. J. Wang, H. Yang, Q. Liu, Q. Liu, X. Li, X. Lv, T. Cheng and H. B. Wu, *ACS Energy Lett.*, 2021, **6**, 437-444.
12. X. Wei, Z. Yin, K. Lyu, Z. Li, J. Gong, G. Wang, L. Xiao, J. Lu and L. Zhuang, *ACS Catal.*, 2020, **10**, 4103-4111.